Rock and Soil Mechanics

Volume 44 | Issue 1 Article 3

3-13-2023

Resilience model for coastal-building foundations with time-variant soil strength due to water intrusion in a changing climate

Cao WANG

School of Civil, Mining and Environmental Engineering, University of Wollongong, Wollongong, Australia

B. M. AYYUB

Center for Technology and Systems Management, Department of Civil and Environmental Engineering, University of Maryland, College Park, Maryland 20742, USA

W. G. P. KUMARI

School of Civil, Mining and Environmental Engineering, University of Wollongong, Wollongong, Australia

Custom Citation

WANG Cao, AYYUB B. M., KUMARI W. G. P. . Resilience model for coastal-building foundations with time-variant soil strength due to water intrusion in a changing climate[J]. Rock and Soil Mechanics, 2023, 44(1): 67-74.

Rock and Soil Mechanics 2023 44(1): 67−74
https: //doi.org/10.16285/j.rsm.2022.00241
ISSN 1000−7598
rocksoilmech.researchcommons.org/journal

Resilience model for coastal-building foundations with time-variant soil strength due to water intrusion in a changing climate

WANG Cao[1], AYYUB B. M.[2], KUMARI W. G. P. [1]

1. School of Civil, Mining and Environmental Engineering, University of Wollongong, Wollongong, Australia
2. Center for Technology and Systems Management, Department of Civil and Environmental Engineering, University of Maryland, College Park, Maryland 20742, USA

Abstract: Groundwater inundation as a consequence of sea level rise triggers significant risks for building foundations in coastal areas. This paper presents a framework to model the resilience of coastal-building foundations in the presence of soil strength deterioration due to water intrusion. The resilience model is mathematically based on the integration of the time-variant performance function within a reference period of interest. A strip foundation is considered, whose ultimate bearing capacity is modeled by the Terzaghi trinomial formula. The rise of groundwater table reduces the strength of soils, and the impact of climate change on groundwater level rise is incorporated in the resilience assessment. An example is presented to demonstrate the applicability of the proposed framework. It is shown that ignoring the effect of water level rise in a changing climate would result in a non-conservative estimate of structural resilience. The life-time resilience is also dependent on the selection of the maintenance strategies, through which the performance function is restored to an enhanced state. Future studies should also consider the joint impact of other factors (e.g., corrosion) on the deterioration of coastal-building foundations.

Keywords: resilience model; coastal-building foundation; time-variant soil strength; water intrusion; climate change

1 Introduction

Building foundations in coastal regions are usually vulnerable to groundwater inundation[1−3]. To ensure the normal serviceability of buildings, the foundations are expected to be resilient, that is, to be in readiness for, to absorb, recover from and adapt to disruptive factors such as water intrusion[4]. It has been projected in the literature[5−6] that the sea level will rise due to the potential impacts of climate change. This will unavoidably lead to groundwater level increase for coastal areas[7], triggering greater failure risks for buildings and constructions[8]. For example, in June 2021, the Champlain Towers South, a 12-story beachfront condominium in Miami, US, partially collapsed[9], and the contributing factors under investigation included the degradation of structural performance due to water penetration. In the presence of these catastrophic events, the question frequently raised was whether a changing climate even exasperated the consequences. In fact, the American Society of Civil Engineers (ASCE) MOP 140 has suggested that[10] new paradigms should be developed for use in engineering practice when climate change may occur but cannot be projected with a high degree of certainty. Manda et al.[1] highlighted the need for groundwater management strategies that address future changes to the groundwater systems in coastal regions. However, urban coastal vulnerability assessments have often overlooked the impact of rising groundwater[11−12].

In the past decades, the engineering community has extended their attention from structural reliability assessment to resilience assessment. For the former, the emphasis is on the safety/serviceability of a structure, typically involving risk analyses[13−14]. For example, Hamrouni et al.[15] performed reliability analysis of the pseudo-static seismic bearing capacity of a strip foundation using the limit equilibrium theory, where the dynamic bearing capacity was determined by modifying the commonly-used static bearing capacity equation. Shen et al.[16] studied the impact of soil spatial variability on the failure mechanism and undrained capacity of strip foundations in a reliability analysis. In terms of resilience assessment, the focus shifts to the life-time continued structural performance under changing conditions[17]. For example, in the design of a geotechnical structure or system, considering reliability alone may be insufficient to fully capture the likelihood, manifestation, and consequences of structural failure states[18]. This is particularly the case when the ever-increasing risks associated with climate change are taken into account[19]. Huang et al.[20] assessed the resilience of a shield tunnel, where the tunnel horizontal convergence was selected as the performance indicator, and a real-world case study of extreme surcharge on Shanghai metro tunnel was presented. Martinez et al.[21]

Received: 22 June 2022 Accepted: 13 September 2022
This work was supported by the Vice-Chancellor's Postdoctoral Research Fellowship from the University of Wollongong, Australia.
First author: WANG Cao, male, born in 1993, PhD, Vice-Chancellor's Postdoctoral Research Fellow, research interests: structural reliability and resilience assessment. E-mail: wangc@uow.edu.au

evaluated the resilience of a representative set of underground transportation assets in coastal areas, where the impacts of sea level rise and storm surge scenarios were assessed. Li et al.[22] developed a resilience model for a degrading anchor-stabilized slope due to corrosion, where maintenance strategies are conducted when the failure probability reaches a predefined threshold. However, limited attention has been paid to the resilience assessment of coastal building foundations exposed to water intrusion.

2 Model for resilience quantification

The concept of resilience includes the following four essential components[23–24]: (1) Robustness–structural ability to withstand hazardous events without significant performance loss; (2) Redundancy–the extent to which the structure remains functional under the impact of disturbance; (3) Resourcefulness–structural ability to diagnose and prioritize problems and to initiate solutions by identifying and mobilizing all types of resources; (4) Rapidity–structural capacity to restore functionality timely. Attoh-Okine et al.[25] proposed a dimensionless measure for structural resilience, Res, as follows,

$$\text{Res} = \frac{1}{t_r - t_h}\int_{t_h}^{t_r} Q(t)\text{d}t \tag{1}$$

in which $Q(t)$ is a function representing structural performance/quality (taking a value between 0 and 1), t_h is the occurrence time of hazard (disruption), and t_r is the time of full recovery. The resilience model in Eq.(1) can be further extended to capture the occurrence of multiple hazardous events. For a reference period of $[0, t_l]$, the life-time resilience measure can be formulated by considering either the summation[26–27] or the multiplication[28–29] of the resilience measures associated with all the hazardous events. In this paper, the former (i.e., summation-based) will be considered, since the focus is on the gradually-varying load capacity of building foundations. Mathematically, the life-time resilience is measured by,

$$\text{Res} = \frac{1}{t_l}\int_0^{t_l} Q(t)\text{d}t \tag{2}$$

where t_l is the duration of service life, and $Q(t)$ is the performance function, which is modeled to be dependent on structural load bearing capacity. Note that there are other forms of resilience definition in the literature[30] except Eq.(1), which can also be used as a basis for structural life-time resilience measure. The resilience measure Res in Eq.(2) varies within [0,1]. In some occasions it is more convenient to use the *nonresilience* measure, which is the complement of Res (i.e., 1 – Res).

The performance function $Q(t)$ being equal to 1.0 means there is no degradation in structural serviceability; on the other hand, $Q(t)$ being 0 indicates no service is available. If the structure suffers from a particular damage state, the structural quality is reduced to β, taking a value between 0 and 1.0, representing the structural deterioration in terms of serviceability. The value of β is dependent on the damage state of the structure, as well as the decision-makers' expertise in practice [31]. For instance, $\beta = 0.8$ means that the building usage is restricted to 80% the normal state. It is straightforward to interpret that, a more severe damage state results in a smaller value of β. In the context of building foundation resilience, the performance function $Q(t)$ is related to the time-variation of the foundation's load bearing capacity. The possible changes in groundwater table, as a result of sea level rise in a changing environment, may trigger damages to the foundation as the resistance degrades to a predefined threshold [32]. For example, in the Chinese Standard for evaluation of existing building subsoil [33], the bearing capacity of foundations can be classified into four grades (A, B, C and D) according to the characteristic ratio c_{ri} (c_{ri} is defined as the ratio of f_a to p_k, where f_a is the characteristic value of the load bearing capacity of ground, and p_k is the average pressure at the foundation bottom under standard load combination): Grade A if $c_{ri} \geqslant 1.0$; B if $0.9 \leqslant c_{ri} < 1$; C if $0.8 \leqslant c_{ri} < 0.9$, and D if $c_{ri} < 0.8$. Corresponding to the evaluation result of the foundation, one may further adjust the utility availability of the building (e.g., fully available, partially available, or not available), which consequently determines the structural performance $Q(t)$. With this regard, an example is presented in the following.

Let R_0 be the initial capacity, and $R(t)$ the degraded capacity at time t. The deterioration of $R(t)$ may be dominated by environmental attacks such as water intrusion, as will be discussed in the next section. The normalized capacity, $R(t)/R_0$, deteriorates gradually from 1 at the initial time (see Fig.1). Before reaching a predefined threshold α_1 at time t_1, the performance function $Q(t)$=1. At the subsequent stage as $R(t)/R_0$ continues to degrade to α_2 at time t_2, the performance function $Q(t)=\beta_1$ (as illustrated in Fig.1). In such a manner until time t_l, $Q(t)$ is described by a step function, depending on the deterioration process of the load bearing capacity. For the case as illustrated in Fig.1, applying Eq.(2), the resilience measure for a service period of $[0, t_l]$ can be calculated by

$$\text{Res} = \frac{1}{t_l}\left[t_1 + (t_2 - t_1)\beta_1 + (t_3 - t_2)\beta_2 + (t_l - t_3)\beta_3\right] \tag{3}$$

Note that in Fig.1, only the gradual deterioration of $R(t)$ has been considered. This model can be further extended to incorporate the impact of shock deteriorations (e.g., due to earthquake excitations).

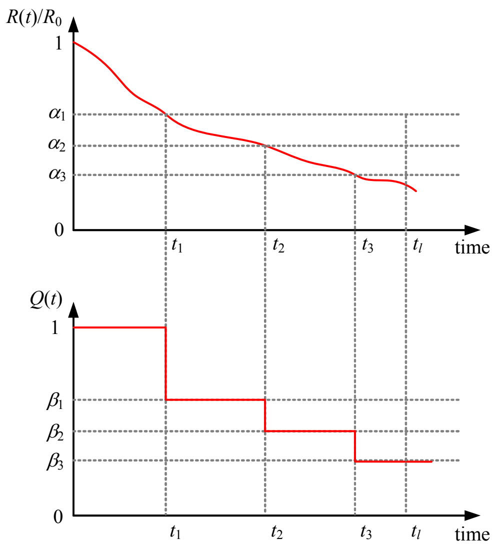

Fig. 1 Dependence of time-variant performance function on deteriorating structural capacity

In the context of structural resilience, if the foundation capacity degrades to an unacceptable level, maintenance measures, such as groundwater drawdown[34], shall be conducted immediately. Fig.2 shows two maintenance strategies. In Fig.2(a), upon $R(t)/R_0$ degrades to α_1 ($0 \leqslant \alpha_1 \leqslant 1$) at time t_i, maintenance measures are taken so that the load bearing capacity is restored to the initial state (it takes a duration of δ_i for the ith maintenance, i=1,2,..., which is referred to as "repair time"). In Fig.2(b), a relatively less strict maintenance strategy is presented, where the intervention is applied when $R(t)/R_0$ degrades to α_2 ($0 \leqslant \alpha_2 \leqslant \alpha_1 \leqslant 1$) at time t_i for i=1,2,... (however, no maintenance measure is taken when $R(t)/R_0$ degrades to α_1 at time t_i'). For both cases in Fig.2, one may employ Eq.(2) to assess the structural life-cycle resilience. Similar to Eq.(3), for the case in Fig.2(a), the resilience measure for a reference period of [0, t_l] can be calculated as follows:

$$\text{Res} = 1 - \frac{1-\beta_1}{t_l}\sum_i \delta_i \tag{4}$$

and for the case in Fig.2(b), the resilience is,

$$\text{Res} = 1 - \frac{1}{t_l}\sum_i\left[(t_i - t_i')(1-\beta_1) + \delta_i(1-\beta_2)\right] \tag{5}$$

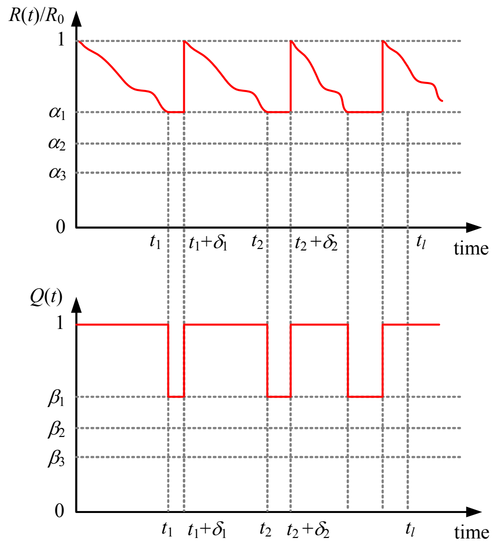

(a) Maintenance measures taken upon $R(t)/R_0$ degrades to α_1

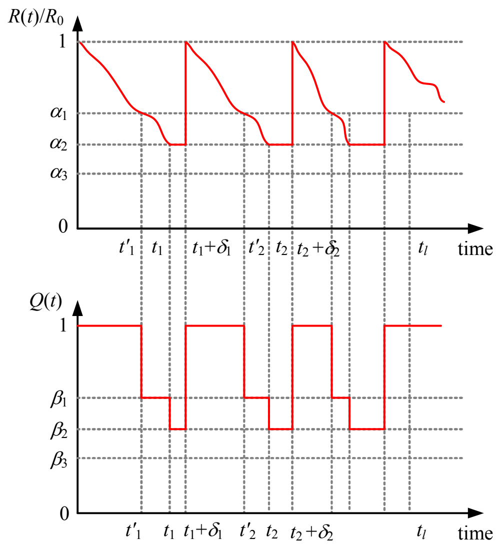

(b) Maintenance measures taken upon $R(t)/R_0$ degrades to α_2

Fig. 2 Dependence of performance function on maintenance strategies

3 Ultimate bearing capacity for strip foundations

In this section, the load bearing capacity of strip foundations will be discussed. To this end, the trinomial formula developed by Terzaghi can be used to calculate the ultimate bearing capacity, q_{ult}, as follows[35],

$$q_{\text{ult}} = cN_c + \gamma D_f N_q + 0.5\gamma B_f N_\gamma \tag{6}$$

where c is the cohesion of soil, γ is the unit weight of soil, D_f and B_f are the depth and width of the foundation, respectively (see Fig.3), N_c 、 N_q and N_γ are non-dimensional bearing capacity factors (functions of the soil internal friction angle, φ), and are defined by

$$\left.\begin{aligned} N_q &= \tan^2\left(\frac{\pi}{4}+\frac{\varphi}{2}\right)\exp(\pi\tan\varphi) \\ N_c &= (N_q-1)\cot\varphi \\ N_\gamma &= 2(N_q+1)\tan\varphi \end{aligned}\right\} \quad (7)$$

Note that other models are also available in the literature[36-38] to compute the ultimate bearing capacity of strip foundations.

The rise of groundwater table may reduce the strength of soils and thus the foundation capacity. In Eq.(6), it has been assumed that the groundwater table is at least at a depth of B_f below the foundation bottom. When this assumption cannot be satisfied, one would need to adjust Eq.(6). As shown in Fig.3, the following two cases are considered[35].

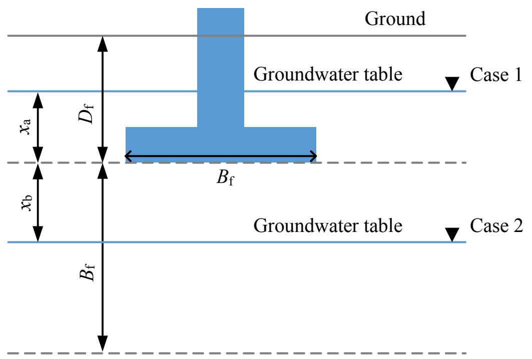

Fig. 3 Illustration of a strip foundation

3.1 Case 1

If the groundwater table is above the foundation bottom, at a distance of x_a, Eq.(6) becomes

$$q_{ult} = cN_c + [\gamma(D_f - x_a) + x_a(\gamma_{sa} - \gamma_w)]N_q + 0.5(\gamma_{sa} - \gamma_w)B_f N_\gamma \quad (8)$$

in which γ_{sa} is the saturated unit weight of soil, γ_w is the unit weight of water, and the remaining variables are as in Eq.(6).

3.2 Case 2

If the groundwater table is below the foundation bottom, at a distance of x_b, Eq.(6) becomes

$$q_{ult} = cN_c + \gamma D_f N_q + 0.5\left[(\gamma_{sa} - \gamma_w) + \frac{x_b}{B_f}(\gamma - \gamma_{sa} - \gamma_w)\right]B_f N_\gamma \quad (9)$$

In order to reflect the impact of sea level rise on groundwater inundation, as shown in Fig.4, assume that the groundwater table relative to the sea level, $h(x)$, at a distance of x to the coastal boundary, can be modeled by the Glover equation as follows[39],

$$h(x) = \sqrt{\frac{2(\rho_s - \rho_f)qx}{\rho_s K}} \quad (10)$$

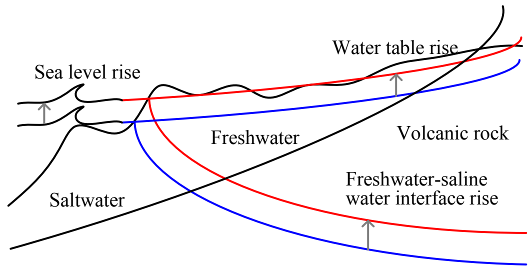

Fig. 4 Groundwater level rise as a consequence of sea level rise (adopted from Ref. [40])

where ρ_s is the saltwater density, ρ_f is the freshwater density, K is the hydraulic conductivity, and q is the freshwater flow per unit length of shoreline. Eq.(10) suggests that for a fixed onshore location (with a fixed value of x), the relative height $h(x)$ is time-invariant. Thus, it is reasonable to assume that the groundwater level rise is equal to that of sea level rise for a particular building site. When evaluating the impact of groundwater level rise on the foundation's ultimate baring capacity, in the presence of Eqs.(6), (8) and (9), with a changing groundwater level, one needs to consider the relative position of the groundwater table with respect to the foundation bottom, so as to choose the appropriate formula to compute the ultimate capacity. In Eqs.(6)−(9), the soil strength parameters (cohesion and internal friction angle) may also vary with time, if taking into account the impacts of bulk density and moisture content[41−42].

4 Example

In this section, a numerical example is presented to demonstrate the applicability of the resilience model in Eq.(2). Consider a strip foundation with a width of 0.9 m and a depth of 0.6 m. The statistical characteristics of the random variables associated with the soil properties are summarized in Table 1. Assume that the foundation is located at a coastal region in Sydney, Australia (Latitude −33.825, Longitude 151.222). According to the Australian Groundwater Explorer Bore ID GW023150, the site is with a high groundwater table[43], which is 1.8 m lower the ground level. Assume that the cohesion of soil c is negligible so that it has a value of zero. The unit weight of water γ_w is 9.81 kN/m^3, and the internal friction angle φ is a time-invariant lognormal variable. It was projected[44] that the global mean sea level may rise 0.5−1.4 m by the end of the 21st century. Thus, in this example, the groundwater table for the foundation site increases linearly by 0.5−1.4 m over a reference period of 80 years.

Table 1 Statistical characteristics of random variables involved in the example

Unit weight of soil γ		Soil friction angle φ		Saturated unit weight of soil γ_{sa}	
Mean /(kN • m^{-3})	Coefficient of variation	Mean /(°)	Coefficient of variation	Mean /(kN • m^{-3})	Coefficient of variation
16	0.15	30	0.10	18	0.15

Fig.5 shows the mean deterioration of the ultimate capacity in time without maintenance measures (denoted by Strategy 0) in the presence of different groundwater level rise scenarios. The results in Fig.5 are obtained through N_s=100,000 replications of simulation, where the statistics in Table 1 are used to generate samples for the random variables. For each case in Fig.5, totally N_s trajectories of time-variant $q_{ult}(t)$ are simulated first, based on which the mean deterioration is obtained by taking the average. It can be seen from Fig.5 that, a more severe sea level rise scenario leads to a greater deterioration rate of the ultimate bearing capacity. If the sea level rises by 0.5 m over 80 years, q_{ult} degrades by 5%; this value is amplified to be 31% if the sea level rises by 1.4 m, suggesting a significantly greater risk of foundation failure. Furthermore, for each case of groundwater rise scenario, the 5th and 95th percentile trajectories are obtained from the N_s samples, and are also presented in Fig.5 to demonstrate the variances associated with the ultimate capacity deterioration processes. With a more severe sea level rise scenario, the deterioration process $q_{ult}(t)$ is associated with a greater uncertainty. For instance, as the sea level rises by 0.5 m, the interval for $q_{ult}(t)/q_{ult}(0)$ featured by the 5th and 95th percentiles is [92.0%, 98.5%] at the end of 80 a. This interval becomes [51.3%, 91.5%] if the sea level rises by 1.4 m.

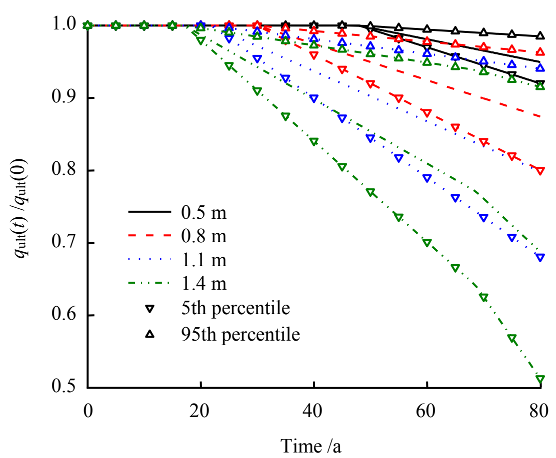

Fig. 5 Deterioration of ultimate bearing capacity $q_{ult}(t)$ with time

As illustrated in Fig.2, in order to achieve a resilient foundation, maintenance measures shall be conducted upon some critical conditions are met. Herein, the following two strategies will be considered.

4.1 Strategy 1

Maintenance measure is conducted immediately when the ultimate bearing capacity decreases to 95% the initial state. The repair time follows a normal distribution with a mean value of 1 a and a COV of 0.2 (see Fig.2(a), with α_1 =0.95).

4.2 Strategy 2

Maintenance measure is conducted when $q_{ult}(t)$ decreases by 10% (i.e., α_2 =0.9 in Fig.2(b)). The repair time is normally distributed with a mean value of 2 a and a COV of 0.2.

It is also assumed that the performance function $Q(t)$ takes a value of 0.8 when $q_{ult}(t)$ reaches α_1 q_{ult} (0) and 0.5 if q_{ult} $(t)/q_{ult}$ (0)=α_2 (i.e., β_1 =0.8, β_2 =0.5). Fig.6 presents sampled trajectories of $Q(t)$ as functions of time associated with different maintenance strategies and sea level rise scenarios. When either strategy 1 or 2 is used, upon the deterioration trajectory of ultimate capacity reaching a damage-defining threshold, the repair time, which is the time the foundation takes to regain initial capacity $q_{ult}(0)$, is simulated based on its statistical characteristics (mean value, COV and distribution type) and is applied to the performance function. The sea level rises by 0.5 m over 80 a in Figs.6(a)−6(c) and 1.4 m in Figs.6(d)−6(f). In Fig.6(a), for each trajectory, when $Q(t)$ decreases from 1 to β_1, due to $q_{ult}(t)/q_{ult}(0)$ reaching α_1, it continues to be β_1 before $q_{ult}(t)/q_{ult}(0)$ reaching α_2, since no maintenance measure is planned. This is different from the cases in Fig.6(b), where the performance function is restored to 1 if $q_{ult}(t)$ degrades to $\alpha_1 q_{ult}(0)$. In Fig.6(c), no maintenance measure is conducted because for all the trajectories, $q_{ult}(t)$ is greater than $\alpha_2 q_{ult}(0)$ due to the relatively slight sea level rise. In Fig.6(d), in the presence of more severe sea level rise scenario (by 1.4 m over 80 a), the performance function, which is described by a step function, degrades with a greater rate compared with that in Fig.6(a). When $q_{ult}(t)$ degrades below $\alpha_2 q_{ult}(0)$, it is assumed that the foundation is in an "unsafe to use" state, and thus the performance function $Q(t)$ equals 0. In Figs.6(e) and 6(f), the performance function is restored to the initial state once $q_{ult}(t)/q_{ult}(0)$ reaches its predefined threshold (α_1 or α_2), which is similar to the illustrations in Fig.2. In the presence of a more severe sea level rise scenario, the restoration measures are conducted more frequently.

Applying Eq.(2), the mean values of foundation nonresilience for a service period of 80 a are summarized in Table 2, considering different maintenance strategies and sea level rise scenarios. The values in Table 2 are obtained through taking the average of 100 000 sampled nonresiliences (random variables) in Eq.(2). Consistent with the observations in Fig.6, a more severe sea level rise results in a larger structural nonresilience (and thus smaller resilience) due to the enhanced risks. Furthermore, with a fixed sea level rise and non-repair measure scenario, the nonresilience associated with strategy 1 is the smallest, followed by those associated with strategy 2 and strategy 0, respectively. This implies that a stricter maintenance strategy (with a greater threshold for the degraded bearing capacity) would lead to a greater structural resilience. This difference is even amplified in the presence of a more severe sea level rise.

The observations from Fig.6 and Table 2 suggest the importance of "adaptive design and adaption" for coastal regions exposed to the impacts of climate change, in particular, sea level rise. The maintenance strategies discussed in this paper align with the recommended action of "accommodation" (i.e., living with the water) in the ASCE MOP 140[10]; other types of adaptions such as "protection" may also be applicable, depending on the available resources. However, designers and engineers should make risk-informed decisions and implement adaptive risk management for coastal building foundations in a changing environment.

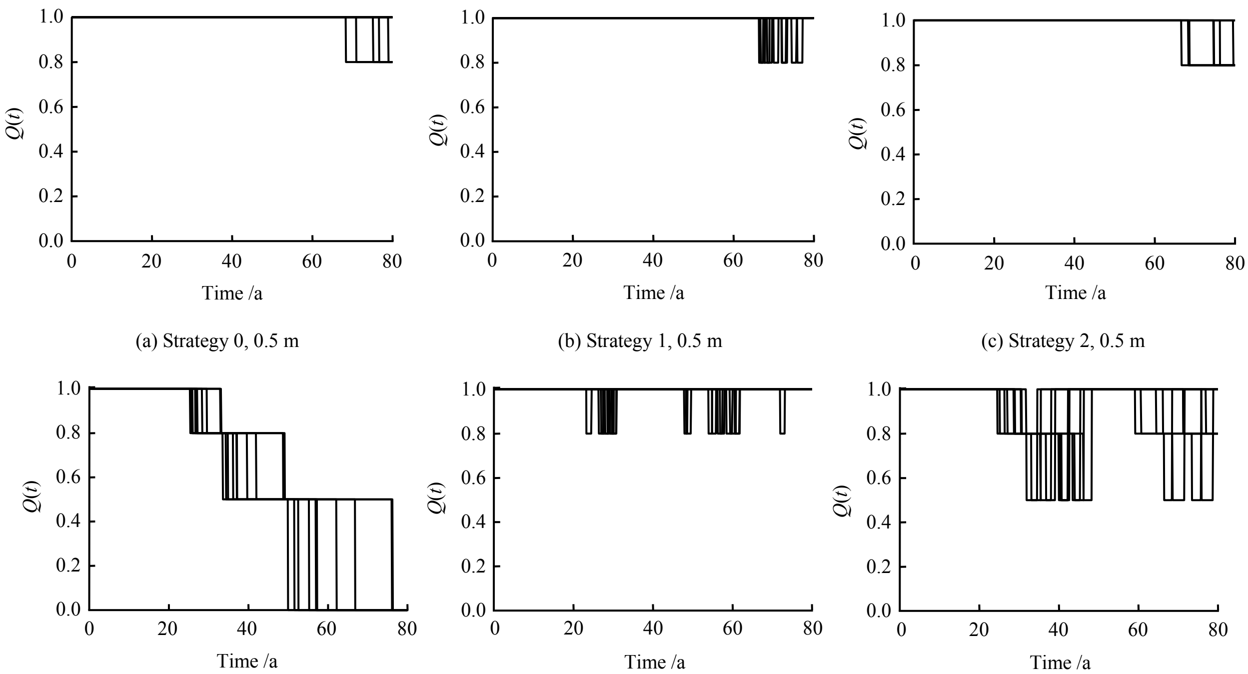

Fig. 6 Sampled trajectories of time-variant performance function

Table 2 Mean value of the nonresilience measure for a reference period of 80 a

Strategy	Mean value of nonresilience measure			
	0.5 m	0.8 m	1.1 m	1.4 m
Strategy 0 (no repair measure)	8.25×10^{-3}	1.10×10^{-1}	2.42×10^{-1}	3.65×10^{-1}
Strategy 1	5.12×10^{-4}	1.64×10^{-3}	3.92×10^{-3}	6.73×10^{-3}
Strategy 2	8.20×10^{-3}	4.87×10^{-2}	4.92×10^{-2}	6.22×10^{-2}

5 Concluding remarks

In this paper, a resilience model for coastal building foundations has been presented. It is based on the integration of the structural performance function within a service period of interest, and takes into account the impact of groundwater intrusion as a consequence of sea level rise in a changing climate, as well as different maintenance strategies. The following conclusions can be made from this paper.

(1) A more severe groundwater level rise results in a larger deterioration rate of foundation ultimate capacity. If the sea level rises by 1.4 m over 80 a, the ultimate bearing capacity could decrease by 31%. This observation suggests the importance of reasonably projecting the future scenarios of groundwater table rise in the design of coastal building foundations.

(2) The selection of maintenance strategy affects the structural resilience significantly. A strategy with a higher maintenance level leads to a smaller structural nonresilience and thus a greater resilience. If the sea level rises by 1.4 m over 80 a, the structural nonresiliences associated with different strategies could vary by one order of magnitude.

Finally, it is noticed that in this paper, only the soil strength deterioration has been discussed. Future works may include the joint impact of corrosion[45] on the capacity of coastal-building foundations.

References

[1] MANDA A K, KLEIN W A. Adaptation strategies to address rising water tables in coastal environments under future climate and sea-level rise scenarios[M]//Coastal Zone Management. Amsterdam: Elsevier, 2019: 403−409.

[2] MALIVA R. Groundwater related impacts of climate change on infrastructure[C]//Climate Change and Groundwater: Planning and Adaptations for a Changing

and Uncertain Future. Cham: Springer, 2021: 177−195.

[3] ABDELHAFEZ M A, ELLINGWOOD B, MAHMOUD H. Hidden costs to building foundations due to sea level rise in a changing climate[J]. Scientific Reports, 2022, 12(1): 1−11.

[4] MCALLISTER T. Developing guidelines and standards for disaster resilience of the built environment: a research needs assessment[R]. Maryland: US Department of Commerce, National Institute of Standards and Technology, 2013.

[5] RIGNOT E, VELICOGNA I, VAN DEN BROEKE M R, et al. Acceleration of the contribution of the Greenland and Antarctic ice sheets to sea level rise[J]. Geophysical Research Letters, 2011, 38: LO5503.

[6] Intergovernmental Panel on Climate Change (IPCC). Climate change: the physical science basis[C]// Contribution of Working Group I to the Sixth Assessment Report of the Intergovernmental Panel on Climate Change. Cambridge: Cambridge University Press, 2021.

[7] BEFUS K M, BARNARD P L, HOOVER D J, et al. Increasing threat of coastal groundwater hazards from sea-level rise in California[J]. Nature Climate Change, 2020, 10(10): 946−952.

[8] KREIBICH H, THIEKEN A H. Assessment of damage caused by high groundwater inundation[J]. Water Resources Research, 2008, 44(9): W09409.

[9] LU X, GUAN H, SUN H, et al. A preliminary analysis and discussion of the condominium building collapse in surfside, Florida, US, June 24, 2021[J]. Frontiers of Structural and Civil Engineering, 2021, 15(5): 1097−1110.

[10] AYYUB B M. Climate-resilient infrastructure: adaptive design and risk management[R]. [S. l.]: American Society of Civil Engineers (ASCE) Committee on Adaptation to a Changing Climate, ASCE Manuals and Reports on Engineering Practice No. 140, 2018.

[11] FU X, PENG Z R. Assessing the sea-level rise vulnerability in coastal communities: a case study in the Tampa Bay Region, US[J]. Cities, 2019, 88: 144-154.

[12] HABEL S, FLETCHER C H, ANDERSON T R, et al. Sea-level rise induced multi-mechanism flooding and contribution to urban infrastructure failure[J]. Scientific Reports, 10, 3796, 2020.

[13] AYYUB B M. Risk analysis in engineering and economics[M]. Boca Raton: Chapman and Hall/CRC, 2003.

[14] WANG C. Structural reliability and time-dependent reliability[M]. Cham: Springer, 2021.

[15] HAMROUNI A, SBARTAI B, DIAS D. Probabilistic analysis of ultimate seismic bearing capacity of strip foundations[J]. Journal of Rock Mechanics and Geotechnical Engineering, 2018, 10(4): 717−724.

[16] SHEN Z, JIN D, PAN Q, et al. Effect of soil spatial variability on failure mechanisms and undrained capacities of strip foundations under uniaxial loading[J]. Computers and Geotechnics, 2021, 139: 104387.

[17] SHAH J, JEFFERSON I, HUNT D. Resilience assessment for geotechnical infrastructure assets[J]. Infrastructure Asset Management, 2014, 1(4): 95−104.

[18] BASU D, MISRA A, PUPPALA A J. Sustainability and geotechnical engineering: perspectives and review[J]. Canadian Geotechnical Journal, 2015, 52(1): 96−113.

[19] LINKOV I, BRIDGES T, CREUTZIG F, et al. Changing the resilience paradigm[J]. Nature Climate Change, 2014, 4(6): 407−409.

[20] HUANG H W, ZHANG D M. Resilience analysis of shield tunnel lining under extreme surcharge: characterization and field application[J]. Tunnelling and Underground Space Technology, 2016, 51: 301−312.

[21] MARTINEZ E, HERNANDEZ J, RODRIGUEZ-NIKL T, et al. Resilience of underground transportation infrastructure in coastal regions: a case study[C]// International Conference on Transportation and Development 2018: Planning, Sustainability, and Infrastructure Systems. Reston: American Society of Civil Engineers, 2018: 223−230.

[22] LI X Y, FAN Z B, LU T, et al. A resilience model for engineered slopes subject to anchor corrosion[J]. KSCE Journal of Civil Engineering, 2018, 22(3): 887−895.

[23] BRUNEAU M, REINHORN A. Exploring the concept of seismic resilience for acute care facilities[J]. Earthquake Spectra, 2007, 23(1): 41−62.

[24] TIERNEY K, BRUNEAU M. Conceptualizing and measuring resilience: a key to disaster loss reduction[J]. TR News, 2007, 250: 14−17.

[25] ATTOH-OKINE N O, COOPER A T, MENSAH S A. Formulation of resilience index of urban infrastructure using belief functions[J]. IEEE Systems Journal, 2009, 3(2): 147−153.

[26] YANG D Y, FRANGOPOL D M. Life-cycle management of deteriorating civil infrastructure considering resilience to lifetime hazards: a general approach based on renewal-reward processes[J]. Reliability Engineering and System Safety, 2019, 183: 197−212.

[27] WANG C, ZHANG H. Assessing the seismic resilience of power grid systems considering the component deterioration and correlation[J]. ASCE-ASME Journal of Risk Uncertainty in Engineering Systems (Part B:

Mechanical Engineering), 2020, 6(2): 020903.

[28] AYYUB B M. Systems resilience for multihazard environments: definition, metrics, and valuation for decision making[J]. Risk Analysis, 2014, 34(2): 340−355.

[29] WANG C, AYYUB B M. Time-dependent resilience of repairable structures subjected to nonstationary load and deterioration for analysis and design[J]. ASCE-ASME Journal of Risk and Uncertainty in Engineering Systems (Part A: Civil Engineering), 2022, 8(3): 04022021.

[30] SHADABFAR M, MAHSULI M, ZHANG Y, et al. Resilience-based design of infrastructure: review of models, methodologies, and computational tools[J]. ASCE-ASME Journal of Risk and Uncertainty in Engineering Systems (Part A: Civil Engineering), 2022, 8(1): 03121004.

[31] LIN P, WANG N. Stochastic post-disaster functionality recovery of community building portfolios I: modeling[J]. Structural Safety, 2017, 69: 96−105.

[32] TOLL D G, ABEDIN Z, BUMA J, et al. The impact of changes in the water table and soil moisture on structural stability of buildings and foundation systems: systematic review CEE10-005 (SR90)[R/OL]. [S. l.]: Collaboration for Environmental Evidence, https://dro.dur.ac.uk/18298/, 2012.

[33] Ministry of Housing and Urban-Rural Development of the People's Republic of China. JGJ/T 404 — 2018 Standard for reliability appraisal of existing building subsoil[S]. Beijing: China Architecture Publishing & Media Co., Ltd., 2018.

[34] SCHWARZ L, REICHL I, KIRSCHNER H, et al. Risks and hazards caused by groundwater during tunnelling: geotechnical solutions used as demonstrated by recent examples from Tyrol[J]. Environmental Geology, 2006, 49(6): 858−864.

[35] DAS B M, SIVAKUGAN N. Principles of foundation engineering[M]. Boston: Cengage Learning, 2018.

[36] AUSILIO E, CONTE E. Influence of groundwater on the bearing capacity of shallow foundations[J]. Canadian Geotechnical Journal, 2005, 42(2): 663−672.

[37] ZHANG C, GAO B, YAN Q, et al. Development of allowable bearing capacity for strip foundations in unsaturated soils[J]. Computers and Geotechnics, 2019, 114: 103138.

[38] CASABLANCA O, BIONDI G, CASCONE E, et al. Static and seismic bearing capacity of shallow strip foundations on slopes[J]. Géotechnique, 2022, 72(9): 769−783.

[39] GLOVER R E. The pattern of freshwater flow in a coastal aquifer[J]. Journal of Geophysical Research, 1959, 64: 457−459.

[40] ROTZOLL K, FLETCHER C H. Assessment of groundwater inundation as a consequence of sea-level rise[J]. Nature Climate Change, 2013, 3(5): 477−481.

[41] MOUAZEN A M, RAMON H, DE BAERDEMAEKER J. Effects of bulk density and moisture content on selected mechanical properties of sandy loam soil[J]. Biosystems Engineering, 2002, 83(2): 217−224.

[42] WEI J, SHI B, LI J, et al. Shear strength of purple soil bunds under different soil water contents and dry densities: a case study in the Three Gorges Reservoir Area, China[J]. Catena, 2018, 166: 124−133.

[43] Bureau of Meteorology, Australia. Australian groundwater explorer, online resource[R/OL]. [S. l.]: [s. n.], http://www. bom.gov.au/water/groundwater/explorer, 2022.

[44] National Research Council, USA. Sea level rise for the coasts of California, Oregon, and Washington: past, present, and future[M]. Washington D.C.: The National Academies Press, 2012.

[45] ZHANG Y, AYYUB B M, FUNG J F. Projections of corrosion and deterioration of infrastructure in United States coasts under a changing climate[J]. Resilient Cities and Structures, 2022, 1(1): 98−109.